

Satellite observation  
of atmospheric  
methane

M. Zou et al.

This discussion paper is/has been under review for the journal Atmospheric Measurement Techniques (AMT). Please refer to the corresponding final paper in AMT if available.

# Satellite observation of atmospheric methane: intercomparison between AIRS and GOSAT TANSO-FTS retrievals

M. Zou<sup>1</sup>, X. Xiong<sup>2,3</sup>, N. Saitoh<sup>4</sup>, J. Warner<sup>5</sup>, Y. Zhang<sup>1</sup>, L. Chen<sup>1</sup>, and F. Weng<sup>3</sup>

<sup>1</sup>The State Key Laboratory of Remote Sensing Science, Institute of Remote Sensing and Digital Earth, Chinese Academy of Sciences, Beijing 100101, China

<sup>2</sup>Earth Resources Technology, Inc, Laurel, MD, USA

<sup>3</sup>NOAA Center for Satellite Applications and Research, College Park, MD 20740, USA

<sup>4</sup>Center for Environmental Remote Sensing, Chiba University, 1-33 Yayoi-cho, Inage-ku, Chiba, Japan

<sup>5</sup>Department of Atmospheric and Oceanic Science, University of Maryland, College Park, MD 20740, USA

Received: 10 August 2015 – Accepted: 17 September 2015 – Published: 14 October 2015

Correspondence to: L. Chen (lfchen@radi.ac.cn)

Published by Copernicus Publications on behalf of the European Geosciences Union.

Title Page

Abstract

Introduction

Conclusions

References

Tables

Figures



Back

Close

Full Screen / Esc

Printer-friendly Version

Interactive Discussion



## Abstract

Space-borne observations of atmospheric methane ( $\text{CH}_4$ ) have been made using the Atmospheric Infrared Sounder (AIRS) on the EOS/Aqua satellite since August 2002 and the Thermal and Near-infrared Sensor for Carbon Observation Fourier Transform Spectrometer (TANSO-FTS) on the Greenhouse Gases Observing Satellite (GOSAT) since April 2009. This study compared the GOSAT TANSO-FTS thermal infrared (TIR) version 1.0  $\text{CH}_4$  product with the collocated AIRS version 6  $\text{CH}_4$  product using data from 1 August 2010 to 30 June 2012, including the  $\text{CH}_4$  mixing ratios and the total column amounts. The results show that at 300–600 hPa, where both AIRS and GOSAT-TIR  $\text{CH}_4$  have peak sensitivities, they agree very well, but GOSAT-TIR retrievals tend to be higher than AIRS in layer 200–300 hPa. At 300 hPa the  $\text{CH}_4$  mixing ratio from GOSAT-TIR is, on average,  $10.3 \pm 31.8$  ppbv higher than that from AIRS, and at 600 hPa GOSAT-TIR retrieved  $\text{CH}_4$  is  $-16.2 \pm 25.7$  ppbv lower than AIRS  $\text{CH}_4$ . Comparison of the total column amount of  $\text{CH}_4$  shows that GOSAT-TIR agrees with AIRS to within 1 % in the mid-latitude regions of Southern Hemisphere and in tropics. In the mid to high latitudes in the Northern Hemisphere, GOSAT-TIR is  $\sim 1$ –2 % lower than AIRS, and in the high-latitude regions of Southern Hemisphere the difference of GOSAT from AIRS varies from  $-3$  % in October to  $+2$  % in July. The difference between AIRS and GOSAT TANSO-FTS retrievals is mainly due to the difference in retrieval algorithms and instruments itself, and the larger difference in the high latitude regions is associated with the low information content and small degree of freedoms of the retrieval. The degree of freedom of GOSAT-TIR retrievals is lower than that of AIRS also indicates that the constraint in GOSAT-TIR retrieval may be too strong. From the good correlation between AIRS and GOSAT-TIR retrievals and the seasonal variation they observed we are confident that the thermal infrared measurements from AIRS and GOSAT-TIR can provide valuable information to capture the spatial and temporal variation of  $\text{CH}_4$ , especially in the mid-upper troposphere, in most time and regions.

## Satellite observation of atmospheric methane

M. Zou et al.

Title Page

Abstract

Introduction

Conclusions

References

Tables

Figures



Back

Close

Full Screen / Esc

Printer-friendly Version

Interactive Discussion



## 1 Introduction

As the third most important long life greenhouse gases after carbon dioxide (CO<sub>2</sub>) and water vapor, atmospheric methane (CH<sub>4</sub>) has a life time of about 12 years, and is more effective in absorbing long-wave radiation as its radiative forcing is about 26 times more than that of CO<sub>2</sub> on a 100 year time horizon, and accounts for 32 % of the total anthropogenic well-mixed greenhouse gas radiative forcing (IPCC, 2013). Mainly attributed to the impact of human activities, the concentration of CH<sub>4</sub> in the atmosphere has increased from the pre-industrial levels of about 700 parts per billion (ppb) to recent level of about 1800–1900 ppb.

Ground-based networks, such as NOAA/ESRL/GMD (National Oceanic and Atmospheric Administration, Earth System Research Laboratory, Global Monitoring Division), provide measurements of CH<sub>4</sub> in the lower troposphere with a high accuracy and long record, but in limited stations. Aircraft measurements from NOAA/ESRL/GMD (Tans, 2009) as well as some research campaigns provide sparse, intermittent measurements of CH<sub>4</sub> vertical profiles. Due to the limited observations in time and space domain, the quantification of CH<sub>4</sub> emission from different sources and in different regions still remains largely uncertain. In recent years, space-borne measurements from satellites have become available, such as the measurements using the thermal infrared (TIR) sensors, which include the Atmospheric InfraRed Sounder (AIRS) on NASA/Aqua (Aumann et al., 2003; Xiong et al., 2008, 2010a, b), Tropospheric Emission Spectrometer (TES) on NASA/Aura (Payne et al., 2009; Wecht et al., 2012; Worden et al., 2012), and the Infrared Atmospheric Sounding Interferometer (IASI) on METOP-A and -B (Xiong et al., 2013; Crevoisiter et al., 2009, 2013; Razavi et al., 2009); measurements using the Near-Infrared (NIR) sensors, which include the SCanning Imaging Absorption spectroMeter for Atmospheric CHartography (SCIAMACHY) instrument onboard ENVISAT for 2003–2009 (Frankenberg et al., 2008, 2011), and the Thermal And Near infrared Sensor for carbon Observation (TANSO) onboard the Greenhouse gases Observation SATellite (GOSAT) from 2009 to present (Yokota et al., 2009; Paker

## Satellite observation of atmospheric methane

M. Zou et al.

Title Page

Abstract

Introduction

Conclusions

References

Tables

Figures



Back

Close

Full Screen / Esc

Printer-friendly Version

Interactive Discussion



et al., 2011; Schepers et al., 2012; Saitoh et al., 2012). These space-borne measurements provide complementary data sources to surface observations for monitoring atmospheric CH<sub>4</sub> with a large spatial and temporal coverage (Kirschke et al., 2013).

Both AIRS, GOSAT TANSO-FTS TIR and other thermal infrared sensors, including TES and IASI, have been used to retrieve atmospheric CH<sub>4</sub>, and these data have been used for analyzing the spatial and temporal variation of CH<sub>4</sub>, so an inter-comparisons of these two different products from AIRS and GOSAT will provide useful information to users to better understand the characteristics of these two products. On the other hand, AIRS V6 CH<sub>4</sub> data were already validated by comparing aircraft data (Xiong et al., 2015), so this comparison of GOSAT data with the “validated” AIRS V6 data is also a kind of indirect validation to GOSAT product, which will give some insight information about the possible over-constraint in GOSAT retrieval algorithm as illustrated later in this paper. This comparison is also a cross-validation to AIRS product, even though their difference can be due to many factors, such as the instruments, radiative transfer models and retrieval algorithms. Section 2 provides a brief introduction of these two instruments, their retrieval algorithms and the data used in this study. Section 3 shows the comparison results, which include the comparison of the retrieved profiles, information contents and the averaging kernels from these two instruments. Both the retrieved CH<sub>4</sub> mixing ratios and the total column amounts in different seasons and different regions are compared. A summary and conclusion are given in Sect. 4.

## 2 CH<sub>4</sub> retrievals from AIRS and GOSAT-TIR

### 2.1 AIRS instrument and the retrieval algorithm description

AIRS on the EOS/Aqua satellite was launched in polar orbit (13:30 LST, ascending node) in May 2002. It has 2378 channels covering 649–1136, 1217–1613 and 2169–2674 cm<sup>-1</sup> at high spectral resolution ( $\lambda/\Delta\lambda = 1200$ ) (Aumann et al., 2003), and the noise in the equivalent change in temperature ( $N\epsilon\Delta T$ ) at a reference temperature of

## Satellite observation of atmospheric methane

M. Zou et al.

Title Page

Abstract

Introduction

Conclusions

References

Tables

Figures



Back

Close

Full Screen / Esc

Printer-friendly Version

Interactive Discussion



---

**Satellite observation  
of atmospheric  
methane**

M. Zou et al.

[Title Page](#)[Abstract](#)[Introduction](#)[Conclusions](#)[References](#)[Tables](#)[Figures](#)[Back](#)[Close](#)[Full Screen / Esc](#)[Printer-friendly Version](#)[Interactive Discussion](#)

250 K ranges from 0.14 K in the 4.2  $\mu\text{m}$  in the lower tropospheric sounding wavelengths to 0.35 K in the 15  $\mu\text{m}$  in the upper tropospheric sounding region. The spatial resolution of AIRS is 13.5 km at nadir, and in a 24 h period, AIRS nominally observes the complete globe twice per day. In order to retrieve  $\text{CH}_4$  in both clear and partially cloudy scenes, 9 AIRS fields-of-views (FOVs) within the footprint of the Advanced Microwave Sounding Unit (AMSU) are used to derive a single cloud-cleared radiance spectrum in a field-of-regard (FOR). The cloud-cleared FOR radiance spectrum is then used to retrieve profiles with a spatial resolution of approximately 45 km. The atmospheric temperature profiles, water vapor profiles, surface temperatures and surface emissivity are required as inputs to compute the radiances in the  $\text{CH}_4$  absorption band. The differences between the computed radiances and the AIRS measured radiances for clear pixels or the derived cloud-cleared FOR radiances for partially cloudy pixels are used to derive  $\text{CH}_4$  profiles. Fifty to sixty  $\text{CH}_4$  absorption channels near 7.66  $\mu\text{m}$  band are selected for the retrievals. The AIRS retrieval algorithm is a sequential retrieval method with multiple steps, in which the temperature and water vapor profiles were retrieved using its own sensitive channels in previous steps, thus the quality of the  $\text{CH}_4$  retrievals depends on the whole AIRS science team's efforts in improving the temperature and moisture profiles as well as surface temperature and emissivity products. More detail of  $\text{CH}_4$  retrievals in its most recent version, i.e. version 6 (V6), can be found in Xiong et al. (2015).

## 2.2 GOSAT TANSO-FTS TIR and the retrieval algorithm description

GOSAT was launched on 23 January 2009 with the primary goal of global observations of column amounts and profiles of  $\text{CO}_2$  and  $\text{CH}_4$  (Yokota et al., 2009). TANSO-FTS on board the GOSAT has TIR bands covering 5.5–14.3  $\mu\text{m}$  with a resolution of 0.2  $\text{cm}^{-1}$  (Kuze et al., 2009). In the TIR retrieval algorithm version 1.0, all the channels in 7.3–8.8  $\mu\text{m}$ , which include both the  $\text{CH}_4$  and  $\text{N}_2\text{O}$  absorption bands, are used for  $\text{CH}_4$  retrieval. The retrieval algorithm is a non-linear maximum a posteriori (MAP) method with linear mapping (Rodgers, 2000). The a priori  $\text{CH}_4$  profiles used in the re-

trieval are taken from the National Institute for Environmental Studies (NIES) transport model (Maksyutov et al., 2008; Saeki et al., 2012). Profiles of temperature and water vapor required for the retrieval are taken from the Japan Meteorological Agency Grid Point Values (JMA-GPV) dataset. Values of surface emissivities are estimated by a linear regression analysis using the Advanced Spaceborne Thermal Emission Reflection Radiometer (ASTER) Spectral Library (Baldrige et al., 2009), the information of land cover, sea ice, wind speed, and the vegetation index derived from the TANSO-Cloud and Aerosol Imager (CAI). Surface temperatures are estimated from the TANSO-FTS TIR spectra in the window region. The signal-to-noise ratios (SNR) of TANSO-FTS at around 7–8  $\mu\text{m}$  band are estimated to be 70–100, and the measurement covariance matrix used in the retrieval is set based on the SNR values. The footprint of GOSAT-TANSO is 10.5 km in diameter, and the number of scan points of GOSAT in cross-track direction is 5 before July 2010, and 3 thereafter.

### 2.3 Data used

This study is made using the standard products of both sensors. GOSAT TANSO-FTS TIR Level 2 CH<sub>4</sub> profile products in version 01.01 for a two-year period from August 2010 to June 2012 are used, and the data during this period has been released to all registered users selected under the GOSAT Research Announcement (RA). AIRS V6 CH<sub>4</sub> data are used in this study and they are downloaded from Goddard Earth Sciences Data and Information Services Center (DISC) (<http://disc.gsfc.nasa.gov/AIRS/index.shtml/>). Only the data from the ascending mode of AIRS, with quality flag equal to 0 or 1, are used for comparison with GOSAT-TIR. Note that the number of retrieval profiles from AIRS is much denser than GOSAT-TIR, as shown in Fig. 1. In this case, the number of profiles from GOSAT-TIR is 1479, while the number of the AIRS profiles from ascending node with QC = 0 and 1 is 164 355. The AIRS retrievals within 1° from each GOSAT-TIR measurement and in the same day were averaged to match-up with each GOSAT-TIR measurement. The errors resulted from the time difference of about 4 h between AIRS and GOSAT-TIR observations were not accounted for in this

## Satellite observation of atmospheric methane

M. Zou et al.

Title Page

Abstract

Introduction

Conclusions

References

Tables

Figures



Back

Close

Full Screen / Esc

Printer-friendly Version

Interactive Discussion



study considering CH<sub>4</sub> is a long residence and well-mixed gas. For simplification, in the comparison of the total column CH<sub>4</sub>, the AIRS gridded products from NASA DISC in 1° × 1° were used directly, and the GOSAT-TIR data was interpolated to the same geographical grid as AIRS.

Comparisons between GOSAT-TIR and AIRS CH<sub>4</sub> products include: (1) CH<sub>4</sub> profile comparison, (2) Comparison of CH<sub>4</sub> mixing ratios with and without using the averaging kernels, and (3) Comparison of the column averaged CH<sub>4</sub> and the total column abundance in different latitude zones and different time. The CH<sub>4</sub> total column abundance from AIRS ascending mode whose unit is molecules cm<sup>-2</sup> was used. Since the unit of GOSAT-TIR CH<sub>4</sub> profile was parts per billion (ppb), we converted it to the total column density using the surface pressure included in the GOSAT-TIR product. As GOSAT TANSO-FTS TIR CH<sub>4</sub> profile consists of 22 layers, and AIRS-V6 CH<sub>4</sub> profile contains 100 layers in the supporting product and 10 layers in the standard product, interpolation of AIRS CH<sub>4</sub> profile from 100 layers to 22 layers was made using the pressure data included in both CH<sub>4</sub> products.

Later in this paper the “differences” between GOSAT-TIR and AIRS CH<sub>4</sub> are calculated as:

$$\Delta X = X_G - X_A$$

or

$$(X_G - X_A)/X_A \times 100\% \quad (1)$$

where X<sub>G</sub> denotes the CH<sub>4</sub> mixing ratios or column amounts from GOSAT-TIR, and X<sub>A</sub> from AIRS.

Satellite observation of atmospheric methane

M. Zou et al.

Title Page

Abstract

Introduction

Conclusions

References

Tables

Figures



Back

Close

Full Screen / Esc

Printer-friendly Version

Interactive Discussion



## 3 Results

### 3.1 Profile comparison

As one example, Fig. 2 shows a simple comparison of the GOSAT-TIR profiles and the match-up AIRS CH<sub>4</sub> profiles from a one-day global data on 4 September 2010. They are in a good agreement overall above 100 hPa and below 400 hPa, but at 200–300 hPa AIRS CH<sub>4</sub> spans a large range and tends to be smaller than GOSAT TIR on average.

The averaging kernels are defined to provide a simple characterization of the relationship between the retrieval and the true state. The retrieval sensitivity can be obtained from the sum of the columns of the averaging kernel matrix, which is also referred to as “the area of the averaging kernel” (Rodgers, 2000). To better demonstrate the differences in sensitivities between AIRS and GOSAT-TIR retrievals, Fig. 3 shows an example of the averaging kernels using data at (38° S, 180° W) on 4 September 2010. There are 10 retrieval layers for AIRS and 22 for GOSAT-TIR. The area of the averaging kernels, which is computed as the sum of all individual kernels, from AIRS is larger than that from GOSAT-TIR, as shown in Fig. 3. To demonstrate the sensitivity variations in latitudes, Fig. 4 shows a curtain plot of the area of averaging kernels using one day data on 4 September 2010. Overall, the patterns from AIRS are similar to GOSAT TIR, with their peak sensitivities located in the 300–600 hPa range in the high latitudes and 200–600 hPa in the tropics. The sensitivities below 800 hPa are small for both, which reflects the major limitation of TIR in measuring the change of CH<sub>4</sub> in the lower troposphere associated with surface emissions.

The information content, which is usually represented as the degree of freedom (DOF), is computed as the trace of the averaging kernel matrix (Rodgers and Connor, 2003). Figure 5 shows the variation of DOFs in different latitudes, and on average, the DOF of AIRS CH<sub>4</sub> is approximately 1.1 whereas the mean of DOFs of GOSAT-TIR CH<sub>4</sub> is approximately 0.61.

Title Page

Abstract

Introduction

Conclusions

References

Tables

Figures



Back

Close

Full Screen / Esc

Printer-friendly Version

Interactive Discussion





## 3.2 Comparison of CH<sub>4</sub> with and without using the averaging kernels

In order to take into account the skill of the CH<sub>4</sub> retrievals, the averaging kernels are usually applied to the “truth” based on the following equation (Rodgers and Connor, 2003):

$$\hat{\mathbf{x}} = \mathbf{A}\mathbf{x} + (\mathbf{I} - \mathbf{A})\mathbf{x}_a \quad (2)$$

where  $\mathbf{I}$  is the identity matrix,  $\mathbf{A}$  is the averaging kernel matrix,  $\mathbf{x}_a$  is the first guess profile for AIRS and the a priori profile for GOSAT-TIR (unit: part per billion volume, ppbv),  $\mathbf{x}$  is the “true” profile, and the computed value of  $\hat{\mathbf{x}}$  is referred to as the convolved data later in this paper, which is usually compared with the retrieved CH<sub>4</sub> mixing ratio in validation studies. Considering the AIRS retrieval layers are coarser than those of GOSAT-TIR and the first guess of AIRS is simple, we used the AIRS averaging kernels,  $\mathbf{A}$ , and AIRS first guess,  $\mathbf{x}_a$  in Eq. (2), to convert the GOSAT-TIR CH<sub>4</sub> profiles,  $\mathbf{x}$ , and the convolved (or smoothed) GOSAT-TIR profiles ( $\hat{\mathbf{x}}$ ) is then compared with AIRS retrieved profiles. As the AIRS averaging kernel is a 10 by 10 matrix, the GOSAT-TIR CH<sub>4</sub> profile and AIRS first guess profile were interpolated into the 10 pressure layers of AIRS retrieval grid when using Eq. (2).

In order to investigate whether the differences between AIRS and GOSAT-TIR retrieved profiles are consistent with their error characteristics and vertical sensitivity, we calculate the error chi-square using Eq. (14) in Rodgers and Connor (2003). Figure 6a shows the RMS of difference (upper panel) and error chi-square (lower panel) of retrieved CH<sub>4</sub> profile from AIRS and GOSAT-TIR. Figure 6b shows the scatter plot of RMS difference vs. error chi-square. The RMS of difference is more than 1.1 times of the error chi-square, and the correlation coefficient  $R^2$  is 0.51, which indicate good consistence.

To show the impact of using averaging kernels in the intercomparison, Fig. 7 shows the scatter plot of AIRS vs. GOSAT-TIR CH<sub>4</sub> mixing ratios in four retrieval layers of 272–343, 343–441, 441–575 and 575–777 hPa. The correlation coefficients between AIRS

and the smoothed GOSAT-TIR values are 0.70, 0.70, 0.79 and 0.87 in these four layers respectively, while the correlation coefficients between AIRS and GOSAT-TIR without smoothing are 0.36, 0.45, 0.57 and 0.75 respectively.

A comparison of the column averaged mixing ratio,  $X_{\text{CH}_4}$ , in Fig. 8 also shows that the correlation coefficient between AIRS and GOSAT TANSO-FTS TIR retrievals increases from 0.88 to 0.91 after using the smoothed data, and the mean difference decreases from  $-21.32$  to  $-2.78$  ppb. The mean difference and standard deviation between AIRS and the smoothed GOSAT-TIR data are smaller than those without smoothing using the averaging kernels, demonstrating that applying the averaging kernels helps achieving better agreements in the intercomparison between two different measurements, as suggested by Rogers and Connor (2003). For simplicity in the next sections we will focus on the direct comparison of the total abundance between AIRS and GOSAT-TIR retrievals.

### 3.3 Comparison of $\text{CH}_4$ total column abundance in different latitude zones

As the sensitivity of TIR measurements is impacted by the surface thermal contrast and the water vapor content in the atmosphere (Deeter et al., 2007; Xiong et al., 2010b), the sensitivity varies with latitudes and seasons. Below we compared the differences between AIRS and GOSAT TANSO-FTS TIR retrieved total column abundance in 6 latitude zones from south to north with an interval of  $30^\circ$ . As shown in Figs. 9 and 10, the correlations between AIRS and GOSAT-TIR are reasonably good, and the correlation coefficient for the least correlated case is 0.83 in zone  $30\text{--}60^\circ\text{S}$ . To show the change of their differences with time, Figs. 9 and 10 also shows the monthly means of the differences from July 2010 to July 2012. In the tropics their differences are less than 1% in all seasons, but in the mid to high latitudes in the Northern Hemisphere, GOSAT-TIR is  $\sim 1 \sim 2\%$  lower than AIRS, with the largest bias occurring in the September. In the high altitudes in the Southern Hemisphere ( $60\text{--}90^\circ\text{S}$ ) the differences of GOSAT from AIRS show a large variation with time, i.e. from  $-3\%$  in October to  $+2\%$  in July. This large difference in the high altitudes in the Southern Hemisphere is related to the very

## Satellite observation of atmospheric methane

M. Zou et al.

Title Page

Abstract

Introduction

Conclusions

References

Tables

Figures



Back

Close

Full Screen / Esc

Printer-friendly Version

Interactive Discussion



low DOFs, particularly in GISAT-TIR retrievals (see Fig. 5), and the large uncertainties in the retrieval of atmospheric states when there are snow/ice coverage over the ocean during October to July.

To better show the difference between GOSAT-TIR and AIRS in different latitudes, we computed the mean difference in a two-year period from 1 August 2010 to 30 June 2012 and in each 15-degree zone. As shown in Fig. 11, the standard deviations in the Southern Hemisphere high latitudes are much larger than in the other latitudes, and the mean differences are smaller from 60° S to 10° N but increases in the north hemisphere to -1.5% at 60° N.

#### 4 Comparison of seasonal cycles from AIRS and GOSAT

Using the monthly-average total column density of CH<sub>4</sub> from AIRS and GOSAT products, we compared the seasonal cycles of CH<sub>4</sub> from 1 August 2010 to 30 June 2012. The left panels in Fig. 12 are the comparisons in the Northern Hemisphere and the right panels are the comparisons in the Southern Hemisphere. Again, GOSAT-TIR agrees with AIRS to within 1% in the mid-latitude regions of Southern Hemisphere and in tropics, however the seasonal variation in the tropics from AIRS observations is larger than that from GOSAT. In the mid to high latitudes in the Northern Hemisphere, GOSAT-TIR is ~1–2% lower than AIRS, but the seasonal variations from them agree well. In the high-latitude regions in Southern Hemisphere, seasonal variation of the total column of CH<sub>4</sub> is large, which is due to a lot of data points with very low total column of CH<sub>4</sub> observed during October–January, however, AIRS and GOSAT agree well in capturing the variation even though their difference is relatively larger than in other regions (see Fig. 10).

### Satellite observation of atmospheric methane

M. Zou et al.

Title Page

Abstract

Introduction

Conclusions

References

Tables

Figures



Back

Close

Full Screen / Esc

Printer-friendly Version

Interactive Discussion



## 5 Summary and conclusions

A thorough comparison of AIRS V6 and GOSAT TANSO-FTS TIR V1.0 CH<sub>4</sub> products using two years data (1 August 2010 to 30 June 2012) has been made. In this comparison, AIRS measurements within a collocation window of 1° by 1° from each GOSAT-TIR measurement in the same day were used. Both the CH<sub>4</sub> mixing ratios and total column amounts have been compared. To understand the differences in the retrievals from these two different instruments, we also compared the differences in the averaging kernels and the DOFs, and examined the use of averaging kernels on the comparison results.

The peak sensitive layers of AIRS and GOSAT-TIR are at similar height, which is at 200–600 hPa in the tropics and 300–600 hPa in the high latitude regions. However, due to the lower SNR of GOSAT TANSO-FTS spectra at 7–8 μm CH<sub>4</sub> band, or over constraint in the GOSAT retrieval algorithm, the degree of freedom of GOSAT-TIR V1.0 retrievals is lower than AIRS.

The comparisons of the profiles showed that the AIRS CH<sub>4</sub> are similar to GOSAT-TIR CH<sub>4</sub>, except AIRS values tend to be lower than GOSAT-TIR at 200–300 hPa. At 300 hPa, the CH<sub>4</sub> mixing ratios from GOSAT are  $10.3 \pm 31.8$  ppbv higher than AIRS, and at 600 hPa, the GOSAT-TIR CH<sub>4</sub> is  $-16.2 \pm 25.7$  ppb lower than AIRS. Between 300–600 hPa, where they have peak sensitivities, AIRS and GOSAT-TIR agree very well. As expected, applying the averaging kernels to smooth the GOSAT-TIR retrievals makes a better agreement between GOSAT with AIRS products.

The comparison of the total column amounts of CH<sub>4</sub> shows that the correlation coefficients between AIRS and GOSAT TANSO-FTS TIR are more than 0.8 in all cases, and the GOSAT-TIR CH<sub>4</sub> agrees with AIRS to within 1 % in the mid-latitudes of the Southern Hemisphere and tropics, but in the mid to high latitudes of the Northern Hemisphere, GOSAT-TIR is ~ 1–2 % lower than AIRS depending on different seasons. In the high latitudes of the Southern Hemisphere the bias varies from –3 % in October to +2 % in July. This large difference in high latitude regions is associated with the low information

### Satellite observation of atmospheric methane

M. Zou et al.

Title Page

Abstract

Introduction

Conclusions

References

Tables

Figures



Back

Close

Full Screen / Esc

Printer-friendly Version

Interactive Discussion



content (or DOF), suggesting a larger uncertainty of retrievals in these regions and a much stricter quality control should be used. We also found AIRS and GOSAT-TIR have a good agreement in capturing the monthly variation of CH<sub>4</sub> density.

In this study, the time difference between AIRS and GOSAT-TIR measurements has not been taken into account. So, the differences, if they could have been measured in the same time, could be slightly smaller than what we presented here. These results demonstrate that the thermal infrared sensors such as AIRS and GOSAT TANSO-FTS TIR can provide valuable consistent information of CH<sub>4</sub> in the mid-upper troposphere. Further comparisons using more recent data as well as direct comparison with aircraft measurements are ongoing.

*Acknowledgements.* This work was supported by the Key Program of the National Natural Science Foundation of China, 41130528 and National Natural Science Foundation of China, 41201353. This study was performed within the framework of the GOSAT Research Announcement.

## References

- Aumann, H. H., Chahine, M. T., Gautier, C., Goldberg, M. D., Kalnay, E., McMillin, L. M., Revercomb, H., Rosenkranz, P. W., Smith, W. L., Staelin, D. H., Strow, L. L., and Susskind, J.: AIRS/AMSU/HSB on the aqua mission: design, science objectives, data products, and processing systems, *IEEE T. Geosci. R.*, 41, 253–264, 2003.
- Baldridge, A. M., Hook, S. J., Grove, C. I., and Rivera, G.: The ASTER spectral library version 2.0, *Remote Sens. Environ.*, 114, 711–715, 2009.
- Crevoisier, C., Nobileau, D., Fiore, A. M., Armante, R., Chédin, A., and Scott, N. A.: Tropospheric methane in the tropics – first year from IASI hyperspectral infrared observations, *Atmos. Chem. Phys.*, 9, 6337–6350, doi:10.5194/acp-9-6337-2009, 2009.
- Crevoisier, C., Nobileau, D., Armante, R., Crépeau, L., Machida, T., Sawa, Y., Matsueda, H., Schuck, T., Thonat, T., Pernin, J., Scott, N. A., and Chédin, A.: The 2007–2011 evolution of tropical methane in the mid-troposphere as seen from space by MetOp-A/IASI, *Atmos. Chem. Phys.*, 13, 4279–4289, doi:10.5194/acp-13-4279-2013, 2013.

## Satellite observation of atmospheric methane

M. Zou et al.

Title Page

Abstract

Introduction

Conclusions

References

Tables

Figures



Back

Close

Full Screen / Esc

Printer-friendly Version

Interactive Discussion



## Satellite observation of atmospheric methane

M. Zou et al.

Title Page

Abstract

Introduction

Conclusions

References

Tables

Figures



Back

Close

Full Screen / Esc

Printer-friendly Version

Interactive Discussion



Deeter, M. N., Edwards, D. P., Gille, J. C., and Drummond, J. R.: Sensitivity of MOPITT observations to carbon monoxide in the lower troposphere, *J. Geophys. Res.*, 112, D24306, doi:10.1029/2007JD008929, 2007.

5 Frankenberg, C., Bergamaschi, P., Butz, A., Houweling, S., Meirink, J. F., Notholt, J., Petersen, A. K., Schrijver, H., Warneke, T., and Aben, I.: Tropical methane emissions: a revised view from SCIAMACHY onboard ENVISAT, *Geophys. Res. Lett.*, 35, L15811, doi:10.1029/2008GL034300, 2008.

10 Frankenberg, C., Aben, I., Bergamaschi, P., Dlugokencky, E. J., Van Hees, R., Houweling, S., Van der Meer, P., Snel, R., and Tol, P.: Global column-averaged methane mixing ratios from 2003 to 2009 as derived from sciamachy: trends and variability, *J. Geophys. Res.*, 116, D04302, doi:10.1029/2010JD014849, 2011.

15 IPCC: Climate Change 2013: The Physical Science Basis. Working Group I Contribution to the Fifth Assessment Report of the Intergovernmental Panel on Climate Change, edited by: Stocker, T. F., Qin, D., Plattner, G.-K., Tignor, M., Allen, S. K., Boschung, J., Nauels, A., Xia, Y., Bex, V., and Midgley, P. M., Cambridge University Press, Cambridge, UK and New York, NY, USA, 1535 p., 2013.

20 Kirschke, S., Bousquet, P., Ciais, P., Saunois, M., Bergamaschi, P., Bruhwiler, L., Canadell, J. G., Chevallier, F., Dlugokencky, E. J., Feng, L., Fraser, A., Heimann, M., Hodson, E., Houweling, S., Josse, B., Lamarque, J.-F., Qu'ere, C. L., Nagashima, T., Naik, V., Palmer, P., Pison, I., Poulter, B., Ringeval, B., Shindell, D. T., Spahni, R., Strode, S. A., Szopa, S., van der Werf, G. R., Voulgarakis, A., and Zeng, G.: Three decades of methane sources and sinks: budgets and variations, *Nat. Geosci.*, 6, 813–823, 2013.

25 Kuze, A., Suto, H., Nakajima, M., and Hamazaki, T.: Thermal and near infrared sensor for carbon observation Fourier-transform spectrometer on the Greenhouse Gases Observing Satellite for greenhouse gases monitoring, *Appl. Optics*, 48, 6716–6733, 2009.

Maksyutov, S., Patra, P. K., Onishi, R., Saeki, T., and Nakazawa, T.: NIES/FRCGC global atmospheric tracer transport model: description, validation, and surface sources and sinks inversion, *J. Earth Sim.*, 9, 3–18, 2008.

30 Parker, R., Boesch, H., Cogan, A., Fraser, A., Feng, L., Palmer, P. I., Messerschmidt, J., Deutscher, N., Griffith, D. W. T., Notholt, J., Wennberg, P. O., and Wunch, D.: Methane observations from the Greenhouse Gases Observing SATellite: comparison to ground-based TCCON data and model calculations, *Geophys. Res. Lett.*, 38, L15807, doi:10.1029/2011GL047871, 2011.

## Satellite observation of atmospheric methane

M. Zou et al.

Title Page

Abstract

Introduction

Conclusions

References

Tables

Figures



Back

Close

Full Screen / Esc

Printer-friendly Version

Interactive Discussion



- Payne, V. H., Clough, S. A., Shephard, M. W., Nassar, R., and Logan, J. A.: Information-centered representation of retrievals with limited degrees of freedom for signal: application to methane from the tropospheric emission spectrometer, *J. Geophys. Res.*, 114, D10307, doi:10.1029/2008JD010155, 2009.
- 5 Razavi, A., Clerbaux, C., Wespes, C., Clarisse, L., Hurtmans, D., Payan, S., Camy-Peyret, C., and Coheur, P. F.: Characterization of methane retrievals from the IASI space-borne sounder, *Atmos. Chem. Phys.*, 9, 7889–7899, doi:10.5194/acp-9-7889-2009, 2009.
- Rodgers, C. D.: *Inverse Methods for Atmospheric Sounding: Theory and Practice*, World Scientific Publishing Co. Pte. Ltd., Singapore, 2000.
- 10 Rodgers, C. D. and Connor, B. J.: Intercomparison of remote sounding instruments, *J. Geophys. Res.*, 108, 4116, doi:10.1029/2002JD002299, 2003.
- Saeki, T., Saito, R., Belikov, D., and Maksyutov, S.: Global high-resolution simulations of CO<sub>2</sub> and CH<sub>4</sub> using a NIES transport model to produce a priori concentrations for use in satellite data retrievals, *Geosci. Model Dev. Discuss.*, 5, 2215–2258, doi:10.5194/gmdd-5-2215-2012, 15 2012.
- Saitoh, N., Touno, M., Hayashida, S., Imasu, R., Shiomi, K., Yokota, T., Yoshida, Y., Machida, T., Matsueda, H., and Sawa, Y.: Comparisons between X<sub>CH<sub>4</sub></sub> from GOSAT shortwave and thermal infrared spectra and aircraft CH<sub>4</sub> measurements over Guam, *Scientific Online Letters on the Atmosphere*, 8, 145–149, doi:10.2151/sola.2012-036, 2012.
- 20 Schepers, D., Guerlet, S., Butz, A., Landgraf, J., Frankenberg, C., Hasekamp, O., Blavier, J. F., Deutscher, N. M., Griffith, D. W. T., Hase, F., Kyro, E., Morino, I., Sherlock, V., Sussmann, R., and Aben, I.: Methane retrievals from Greenhouse Gases Observing Satellite (GOSAT) shortwave infrared measurements: performance comparison of proxy and physics retrieval algorithms, *J. Geophys. Res.*, 117, D10307, doi:10.1029/2012jd017549, 2012.
- 25 Tans, P. P.: The atmospheric buildup rate for carbon is based on measurements of CO<sub>2</sub> at Mauna Loa obtained by the NOAA Earth System Research Laboratory, available at: ftp://aftp.cmdl.noaa.gov/products/trends/co2/co2\_gr\_mlo.txt, www.esrl.noaa.gov/gmd/ccgg/trends/ (last access: 5 October 2015), 2009.
- Wecht, K. J., Jacob, D. J., Wofsy, S. C., Kort, E. A., Worden, J. R., Kulawik, S. S., Henze, D. K., Kopacz, M., and Payne, V. H.: Validation of TES methane with HIPPO aircraft observations: implications for inverse modeling of methane sources, *Atmos. Chem. Phys.*, 12, 1823–1832, doi:10.5194/acp-12-1823-2012, 2012.
- 30

**Satellite observation  
of atmospheric  
methane**

M. Zou et al.

Title Page

Abstract

Introduction

Conclusions

References

Tables

Figures



Back

Close

Full Screen / Esc

Printer-friendly Version

Interactive Discussion



- Worden, J., Kulawik, S., Frankenberg, C., Payne, V., Bowman, K., Cady-Peirara, K., Wecht, K., Lee, J.-E., and Noone, D.: Profiles of CH<sub>4</sub>, HDO, H<sub>2</sub>O, and N<sub>2</sub>O with improved lower tropospheric vertical resolution from Aura TES radiances, *Atmos. Meas. Tech.*, 5, 397–411, doi:10.5194/amt-5-397-2012, 2012.
- 5 Xiong, X., Barnet, C., Maddy, E., Sweeney, C., Liu, X., Zhou, L., and Goldberg, M.: Characterization and validation of methane products from the Atmospheric Infrared Sounder (AIRS), *J. Geophys. Res.*, 113, G00A01, doi:10.1029/2007JG000500, 2008.
- Xiong, X., Barnet, C., Maddy, E., Wei, J., Liu, X., and Pagano, T. S.: Seven years' observation of mid-upper tropospheric methane from atmospheric infrared sounder, *Remote Sens.*, 2, 2509–2530, 2010a.
- 10 Xiong, X., Barnet, C. D., Zhuang, Q., Machida, T., Sweeney, C., and Patra, P. K.: Mid-upper tropospheric methane in the high Northern Hemisphere: spaceborne observations by AIRS, aircraft measurements, and model simulations, *J. Geophys. Res.*, 115, D19309, doi:10.1029/2009JD013796, 2010b.
- 15 Xiong, X., Barnet, C., Maddy, E. S., Gambacorta, A., King, T. S., and Wofsy, S. C.: Mid-upper tropospheric methane retrieval from IASI and its validation, *Atmos. Meas. Tech.*, 6, 2255–2265, doi:10.5194/amt-6-2255-2013, 2013.
- Xiong, X., Weng, F., Liu, Q., and Olsen, E.: Space-borne observation of methane from atmospheric infrared sounder version 6: validation and implications for data analysis, *Atmos. Meas. Tech. Discuss.*, 8, 8563–8597, doi:10.5194/amt-d-8-8563-2015, 2015.
- 20 Yokota, T., Yoshida, Y., Eguchi, N., Ota, Y., Tanaka, T., Watanabe, H., and Maksyutov, S.: Global concentrations of CO<sub>2</sub> and CH<sub>4</sub> retrieved from GOSAT: first preliminary results, *Scientific Online Letters on the Atmosphere*, 5, 160–163, 2009.



Satellite observation  
of atmospheric  
methane

M. Zou et al.

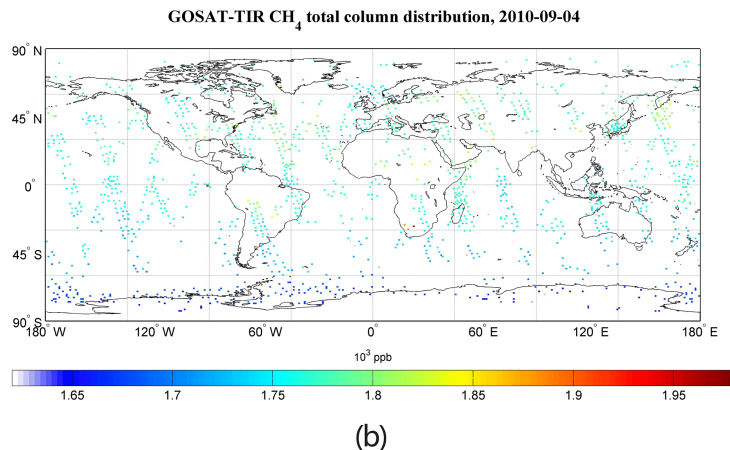
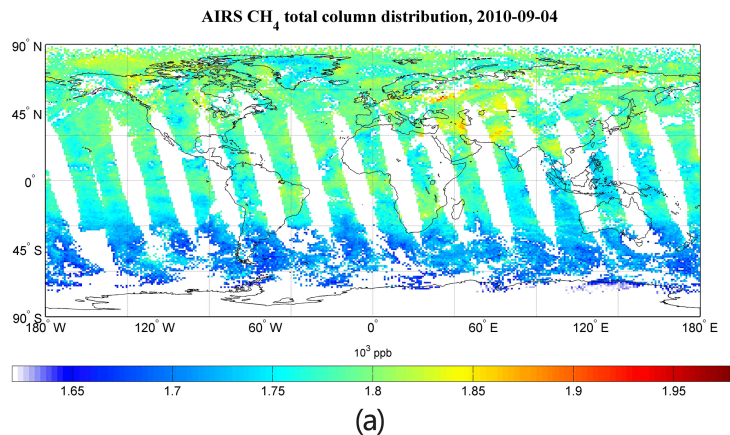


**Figure 1.** Much larger coverage of AIRS retrievals **(a)** as compared to GOSAT TANSO-FTS **(b)** as shown from the global CH<sub>4</sub> total column density on 4 September 2010. AIRS data from ascending mode with QC = 0, 1 are plotted.

Title Page

Abstract

Introduction

Conclusions

References

Tables

Figures

◀

▶

◀

▶

Back

Close

Full Screen / Esc

Printer-friendly Version

Interactive Discussion



**Satellite observation  
of atmospheric  
methane**

M. Zou et al.

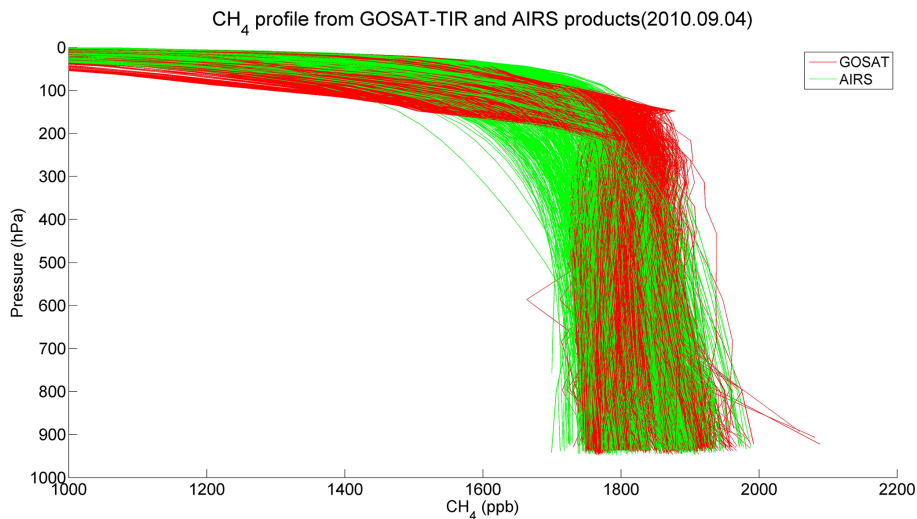


**Figure 2.** Comparison of the match-up AIRS CH<sub>4</sub> profiles vs. the GOSAT-TIR profiles using one day global data on 4 September 2010.  $N = 1182$ .

[Title Page](#)[Abstract](#)[Introduction](#)[Conclusions](#)[References](#)[Tables](#)[Figures](#)[◀](#)[▶](#)[◀](#)[▶](#)[Back](#)[Close](#)[Full Screen / Esc](#)[Printer-friendly Version](#)[Interactive Discussion](#)

## Satellite observation of atmospheric methane

M. Zou et al.

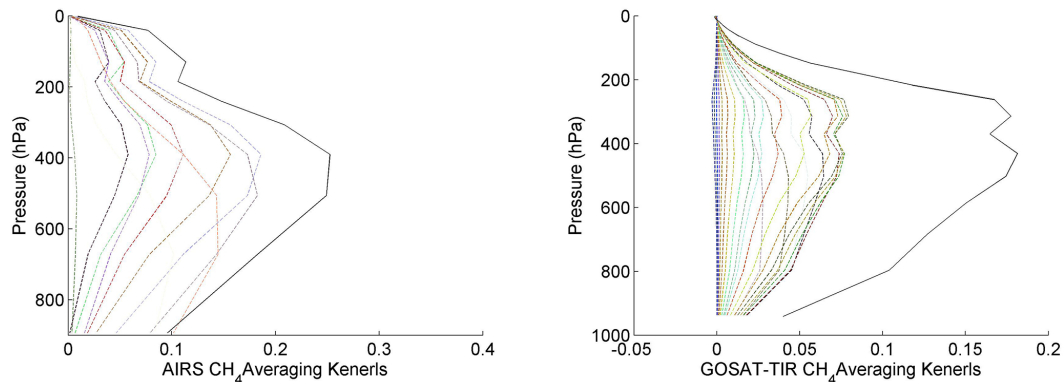


**Figure 3.** The averaging kernels of AIRS and GOSAT TANSO-FTS TIR V1.0 CH<sub>4</sub> retrievals on 4 September 2010. There are 10 dash lines for AIRS retrievals and 22 dash lines for GOSAT retrievals, corresponding to the retrieval layers used in each of them. The black solid line is the area of kernels divided by 4.

Title Page

Abstract

Introduction

Conclusions

References

Tables

Figures

◀

▶

◀

▶

Back

Close

Full Screen / Esc

Printer-friendly Version

Interactive Discussion



**Satellite observation  
of atmospheric  
methane**

M. Zou et al.

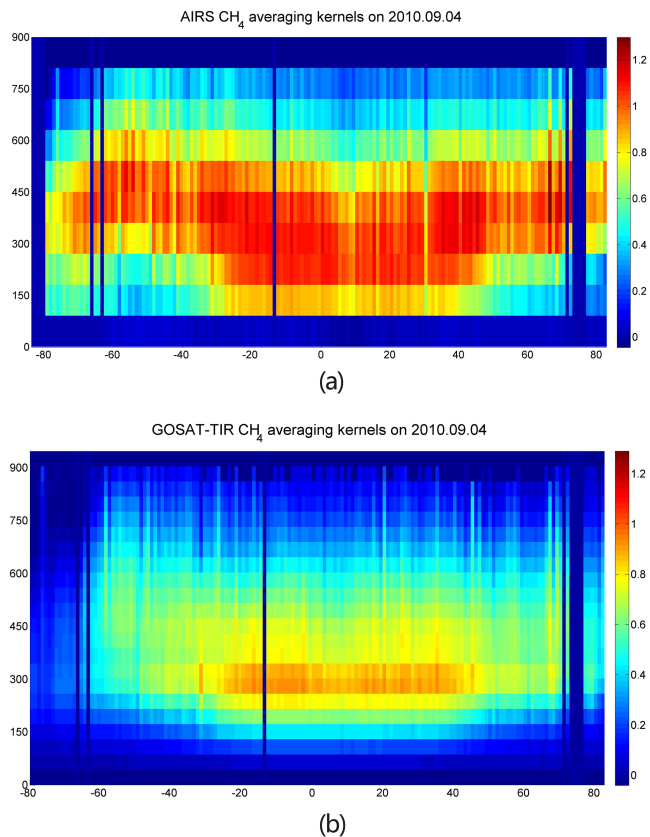


**Figure 4.** The area of the averaging kernels of CH<sub>4</sub> retrievals from **(a)** AIRS and **(b)** GOSAT TANSO-FTS V1.0 TIR observations in different latitudes on 4 September 2010.

[Title Page](#)[Abstract](#)[Introduction](#)[Conclusions](#)[References](#)[Tables](#)[Figures](#)[◀](#)[▶](#)[◀](#)[▶](#)[Back](#)[Close](#)[Full Screen / Esc](#)[Printer-friendly Version](#)[Interactive Discussion](#)

**Satellite observation  
of atmospheric  
methane**

M. Zou et al.

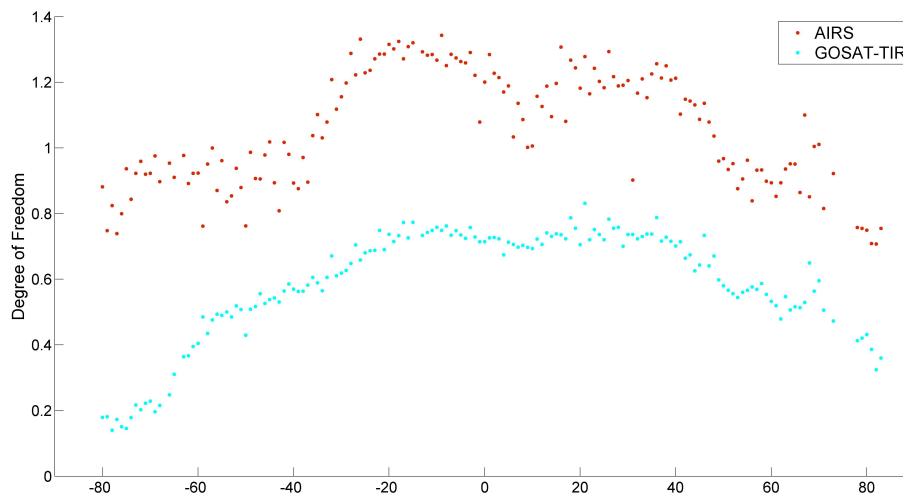


**Figure 5.** Latitudinal variation of DOF for AIRS and GOSAT TANSO-FTS V1.0 CH<sub>4</sub> retrievals on 4 September 2010.

[Title Page](#)[Abstract](#)[Introduction](#)[Conclusions](#)[References](#)[Tables](#)[Figures](#)[Back](#)[Close](#)[Full Screen / Esc](#)[Printer-friendly Version](#)[Interactive Discussion](#)

Satellite observation  
of atmospheric  
methane

M. Zou et al.

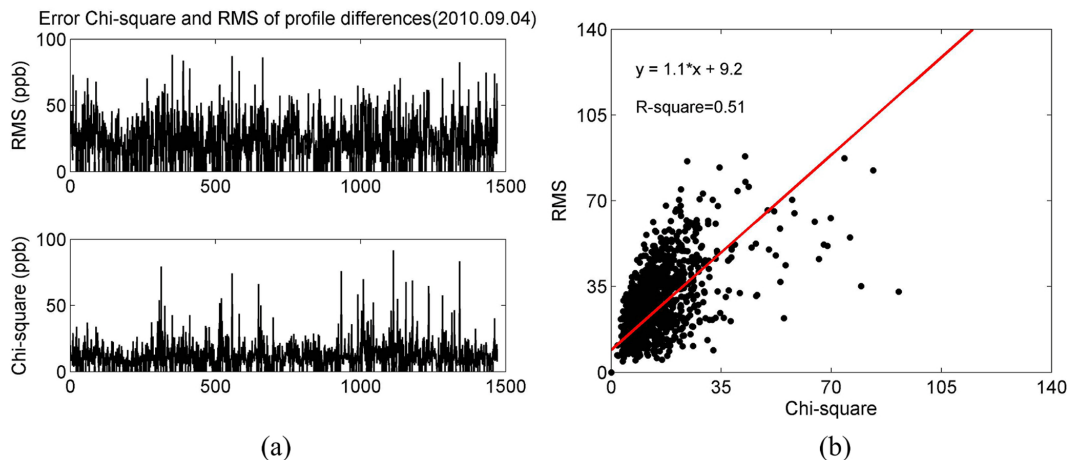


**Figure 6.** Comparison of the RMS difference and error chi-square of retrieved CH<sub>4</sub> profiles from AIRS and GOSAT-TIR. **(a)** The upper panel shows the RMS of CH<sub>4</sub> profile difference and the lower panel is the error chi-square, **(b)** the scatter plot of RMS difference and error chi-square.

[Title Page](#)[Abstract](#)[Introduction](#)[Conclusions](#)[References](#)[Tables](#)[Figures](#)[Back](#)[Close](#)[Full Screen / Esc](#)[Printer-friendly Version](#)[Interactive Discussion](#)

Satellite observation  
of atmospheric  
methane

M. Zou et al.

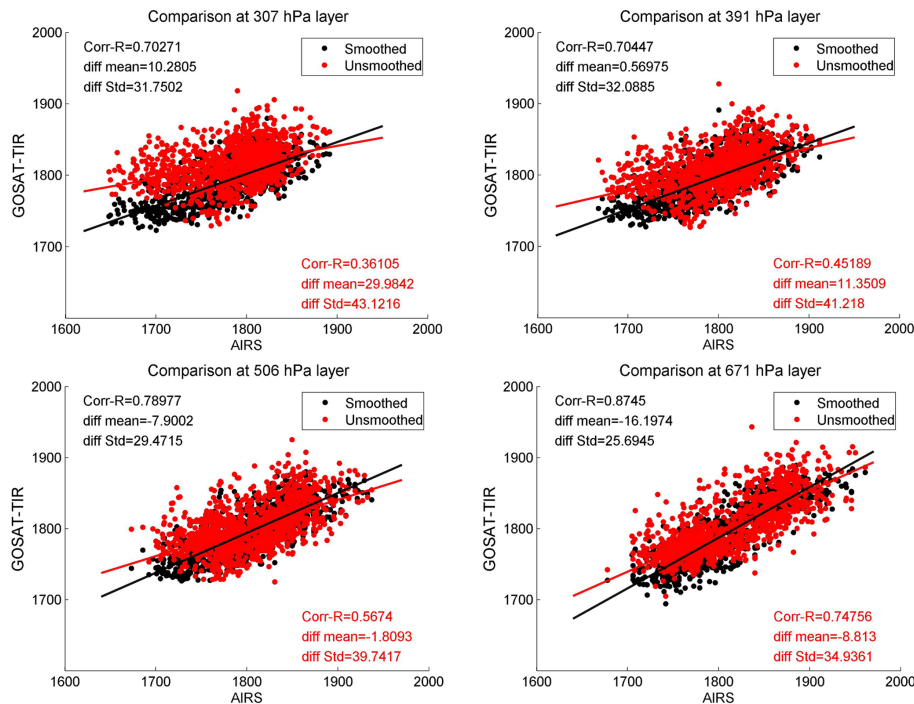


**Figure 7.** Comparisons of AIRS and GOSAT TANSO-FTS TIR smoothed  $\text{CH}_4$  at four retrievals levels of 272–343, 343–441, 441–575 and 575–777 hPa (the mean effective pressures are 307, 391, 506 and 671 hPa respectively).

## Satellite observation of atmospheric methane

M. Zou et al.

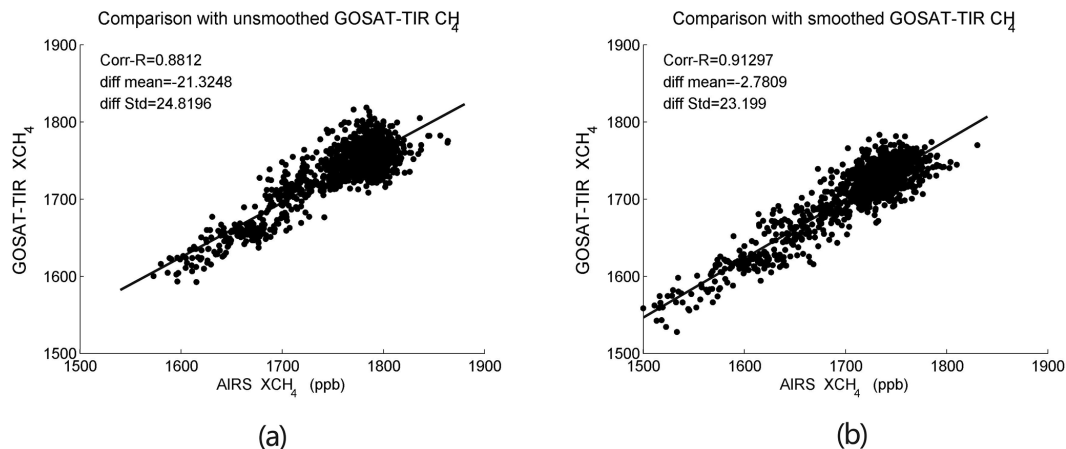


**Figure 8.** Comparison of  $X_{\text{CH}_4}$  between AIRS and **(a)** unsmoothed GOSAT TANSO-FTS TIR  $X_{\text{CH}_4}$  and **(b)** smoothed GOSAT-TIR  $X_{\text{CH}_4}$  using AIRS averaging kernel. Global data on 4 September 2010 are used.

Title Page

Abstract

Introduction

Conclusions

References

Tables

Figures



Back

Close

Full Screen / Esc

Printer-friendly Version

Interactive Discussion





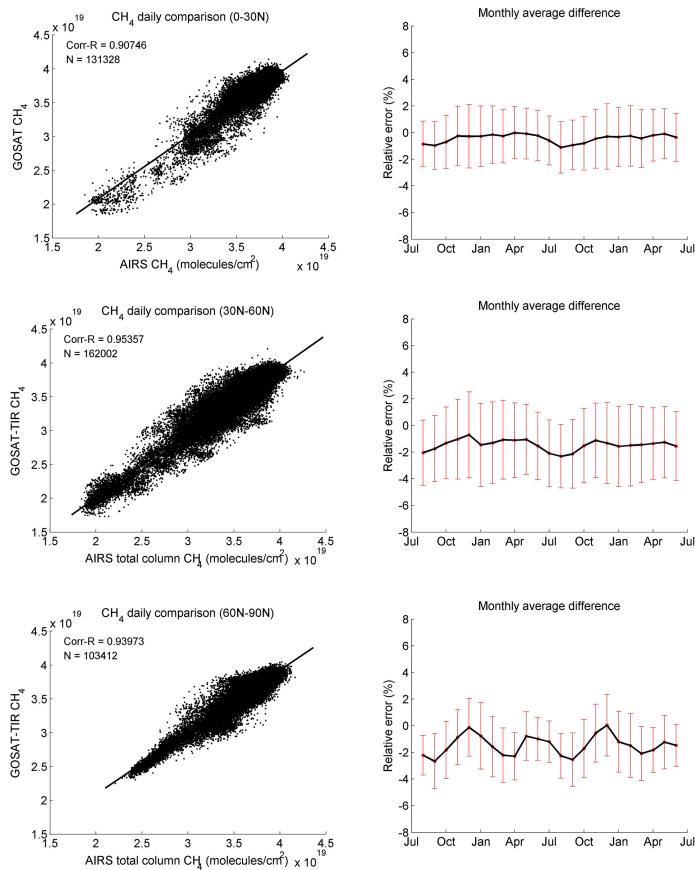


**Figure 9.** Scatter plot of AIRS vs. GOSAT TANSO-FTS TIR CH<sub>4</sub> total column density over 3 latitude zones in the Northern Hemisphere using data from 1 August 2010 to 30 June 2012 (left panels). Right panels show the variation of the mean difference  $r$  in each month, and the bars are the standard deviation.

**Satellite observation of atmospheric methane**

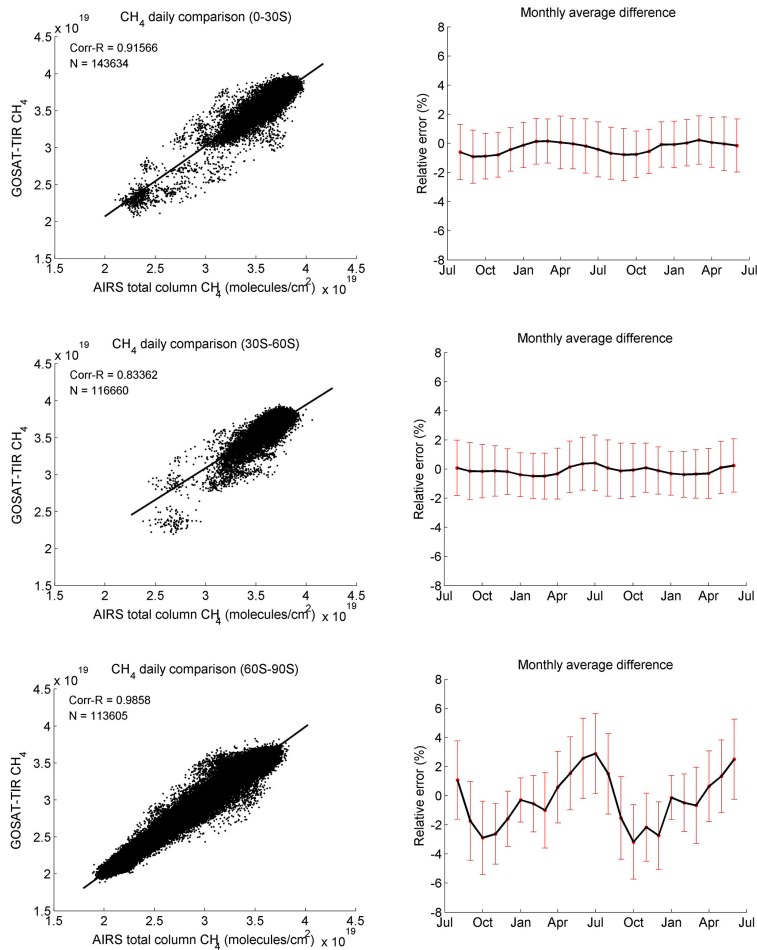
M. Zou et al.

Title Page	
Abstract	Introduction
Conclusions	References
Tables	Figures
◀	▶
◀	▶
Back	Close
Full Screen / Esc	
Printer-friendly Version	
Interactive Discussion	



## Satellite observation of atmospheric methane

M. Zou et al.



Title Page	
Abstract	Introduction
Conclusions	References
Tables	Figures
◀	▶
◀	▶
Back	Close
Full Screen / Esc	
Printer-friendly Version	
Interactive Discussion	

**Figure 10.** Same as Fig. 8 but for 3 latitude zones in the Southern Hemisphere.



**Satellite observation  
of atmospheric  
methane**

M. Zou et al.

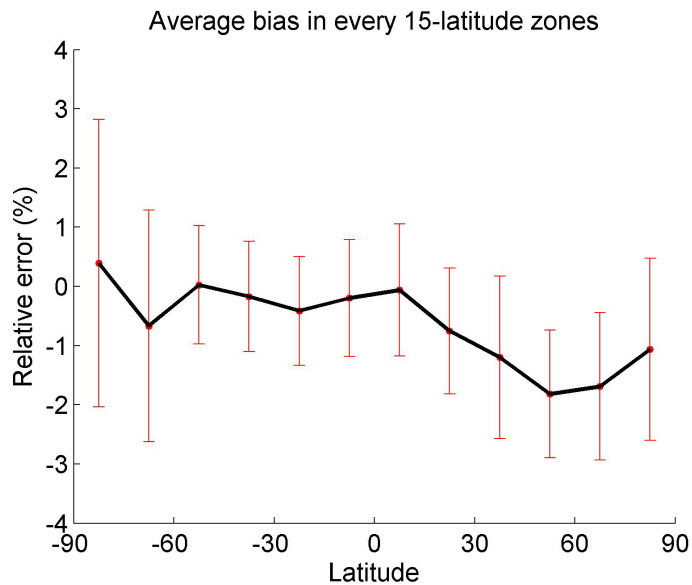


**Figure 11.** Errors of GOSAT-TIR total column  $\text{CH}_4$  relative to AIRS total column  $\text{CH}_4$  in different latitude using data from 1 August 2010 to 30 June 2012.

[Title Page](#)[Abstract](#)[Introduction](#)[Conclusions](#)[References](#)[Tables](#)[Figures](#)[◀](#)[▶](#)[◀](#)[▶](#)[Back](#)[Close](#)[Full Screen / Esc](#)[Printer-friendly Version](#)[Interactive Discussion](#)

## Satellite observation of atmospheric methane

M. Zou et al.

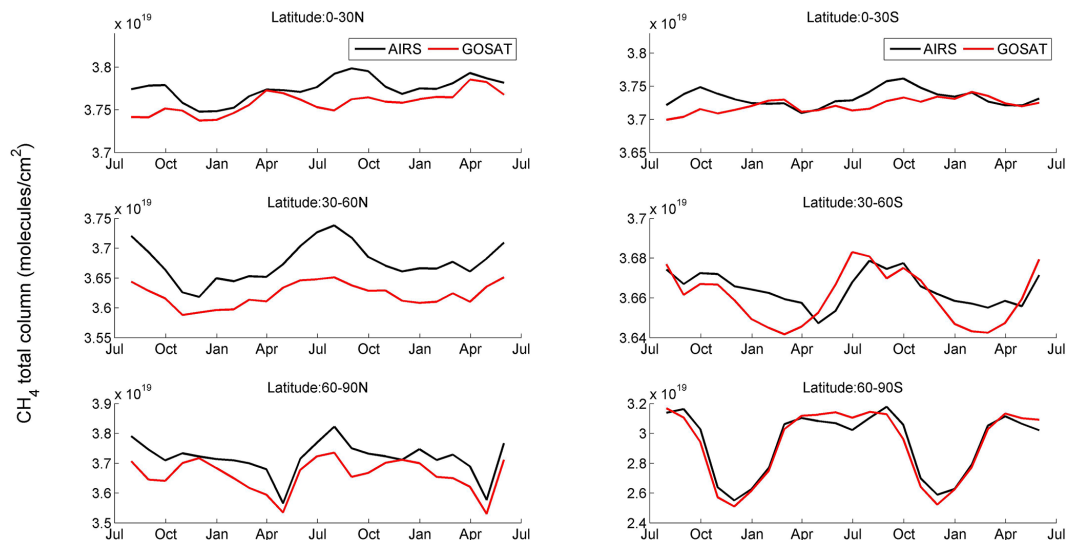


**Figure 12.** Trends of  $\text{CH}_4$  monthly-average total column amounts in different latitudes using AIRS and GOSAT-TIR products from 1 August 2010 to 30 June 2012. The left panels are the comparison in the Northern Hemisphere and the right panels are the comparison in the Southern Hemisphere.

[Title Page](#)
[Abstract](#)
[Introduction](#)
[Conclusions](#)
[References](#)
[Tables](#)
[Figures](#)
[⏪](#)
[⏩](#)
[◀](#)
[▶](#)
[Back](#)
[Close](#)
[Full Screen / Esc](#)
[Printer-friendly Version](#)
[Interactive Discussion](#)
